

# RANDOM PROJECTIONS FOR ADVERSARIAL ATTACK DETECTION

**Nathan Drenkow & Neil Fendley & Philippe Burlina \***

The Johns Hopkins University Applied Physics Laboratory  
Laurel, MD 20723, USA

## ABSTRACT

Whilst adversarial attack detection has received considerable attention, it remains a fundamentally challenging problem from two perspectives. First, while threat models can be well-defined, attacker strategies may still vary widely within those constraints. Therefore, detection should be considered as an open-set problem, standing in contrast to most current detection strategies. These methods take a closed-set view and train binary detectors, thus biasing detection toward attacks seen during detector training. Second, information is limited at test time and confounded by nuisance factors including the label and underlying content of the image. Many of the current high-performing techniques use training sets for dealing with some of these issues, but can be limited by the overall size and diversity of those sets during the detection step. We address these challenges via a novel strategy based on random subspace analysis. We present a technique that makes use of special properties of random projections, whereby we can characterize the behavior of clean and adversarial examples across a diverse set of subspaces. We then leverage the self-consistency (or inconsistency) of model activations to discern clean from adversarial examples. Performance evaluation demonstrates that our technique outperforms ( $> 0.92$  AUC) competing state of the art (SOTA) attack strategies, while remaining truly agnostic to the attack method itself. It also requires significantly less training data, composed only of clean examples, when compared to competing SOTA methods, which achieve only chance performance, when evaluated in a more rigorous testing scenario.

## 1 INTRODUCTION

The rise of deep learning has led to state-of-the-art advances in machine learning (ML) across almost every conceivable application. With deep neural networks (DNNs) as the core computational elements in increasingly complex ML systems, there is greater demand than ever for an improved understanding of how these networks function. In particular, there is an ever-growing need to understand DNN vulnerabilities, failure modes, and performance shortcomings as well as the mechanisms and environmental conditions that create these challenges.

The discovery of adversarial examples (Goodfellow et al. (2014)) has led to a wide range of subsequent findings in domains such as image classification, object detection, natural language processing, speech processing, and reinforcement learning. In a sense, an adversarial arms race has developed wherein researchers find themselves into a continuous cycle of development of methods for attacks and defenses. A core problem in adversarial machine learning (AML), from both the attack and defense perspectives, is the determination of model robustness in this context. While adversarial examples are realized in the input domain, their intended and ultimate effect is on model behavior. As such, we focus on developing a model-centric method of adversarial example (AE) detection.

---

\*Primary POC: Nathan Drenkow (nathan.drenkow@jhupl.edu)

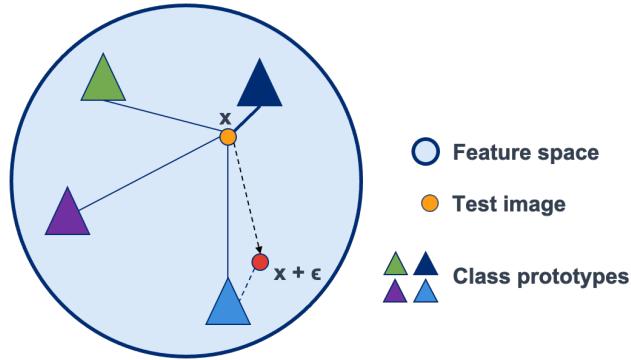


Figure 1: Distances in feature space between an image embedding and class prototypes are used as a proxy for predicting class labels. Adversarial perturbations shift the clean representation such that the distance to the true class prototype increases and the distance to the incorrect prototype decreases.

## 2 RELATED WORK - ADVERSARIAL EXAMPLE DETECTION

While developing novel attack and defense strategies occupies a large proportion of past AML research work, interest in automated detection of adversarial examples has grown considerably in recent years. In many respects, adversarial detection is a complementary problem to adversarial defense, but we focus here on efforts to explicitly identify cases of adversarial manipulation and leave it to downstream methods to mitigate the effects of any such manipulations.

We find the bulk of the AE detection work falls roughly into the following categories:

- **Input-space detection** - Methods that seek to identify adversarial examples through an examination/manipulation of the inputs to DNNs (Liang et al. (2018); Tian et al. (2018); Xu et al. (2017)).
- **Feature-space detection** - Methods which typically train new models on intermediate or final DNN layer outputs (Metzen et al. (2017); Bagnall et al. (2017); Crecchi et al. (2019); Wang et al. (2019); Fidel et al. (2019); Abdelzaher et al. (2018); Miller et al. (2017); Papernot & McDaniel (2018); Roth et al. (2019); Ma et al. (2018c); Feinman et al. (2017)).
- **Robustness Certificates** - Theoretical proofs for DNN robustness under specific threat models (assumptions for both attacker and defender) (Wong & Kolter (2018); Raghunathan et al. (2018); Weng et al. (2018, 2019); Wang et al. (2019); Singla & Feizi (2019); Levine & Feizi (2019); Lyu et al. (2019); Kumar et al. (2020); Lecuyer et al. (2019); Boopathy et al. (2019); Gehr et al. (2018)).
- **Statistical Detection** - Methods that focus on generating robust test statistics that separate clean from adversarial examples (Li & Li (2017); Grosse et al. (2017); Quintanilha et al. (2018)).
- **Network Coverage** - Methods that examine neuron coverage as a means to test DNN behavior and potentially establish differences between clean and adversarial examples (Ma et al. (2018a;b); Sun et al. (2018b;a); Pei et al. (2017)).

Of specific relevance to our approach, are a set of high-performing methods (Lee et al. (2018); Ma et al. (2018c); Feinman et al. (2017); Papernot & McDaniel (2018)) which use local latent space geometry for AE detection. The work by Feinman et al. (2017) originally combined kernel density estimation and Bayesian uncertainty estimation to identify AEs as predicted-class outliers. The work by Lee et al. (2018) provided a similar view but through the lens of Gaussian Discriminant Analysis to estimate class confidence scores based on Mahalanobis distance (combined with a layer-wise logistic regression model to predict AE likelihood).

Ma et al. (2018c); Papernot & McDaniel (2018) perform AE detection through nearest-neighbor principles where Ma et al. (2018c) relies on Local Intrinsic Dimensionality (LID) to characterize

local neighborhood structure while Papernot & McDaniel (2018) uses discrete k-Nearest Neighbors along with conformal prediction to identify neighborhood (in)consistencies. Our approach is inspired by elements of these papers and in particular, the approach towards AE detection looking at (in)consistencies in latent-space behavior for both adversarial and clean examples.

### 3 NOVEL CONTRIBUTIONS

We present a novel approach to AE detection which uses a form of subspace analysis to differentiate between model behavior under clean and adversarial conditions. Additional advantages and novel features of our proposed approach are as follows:

- Our detection scheme uses random projection subspaces to compare and analyze network activation behavior in a self-supervised manner.
- While most SOTA methods require some prior knowledge of attacks to train their detectors, our method is truly attack-agnostic and requires a training set composed solely of clean examples.
- Additionally, while most methods rely on large training datasets, our method is extremely data efficient and requires only a fraction of the training data typically used for adversarial detection. Our experiments show that training data requirements scale according to the complexity of the problem (e.g., number of classes) rather than the detection method itself.
- Last, we evaluate our method under much more rigorous constraints than are typical used, by significantly reducing the size of the training set and restricting its composition to clean examples only (a true attack-agnostic training paradigm). Under these more difficult conditions, our method far outperforms comparable methods across a variety of unseen attacks.

### 4 BACKGROUND AND NOTATION

We first provide some basic notation and assumptions. In typical classification tasks, we start from a set of exemplars  $(x, y)$  where  $x \in \mathcal{X} = \{\text{all possible inputs}\}$  and  $y \in Y = \{1, \dots, K\}$  (with  $K$  being the number of classes). The aim is to produce a model,  $f : X \rightarrow Y$ , which minimizes some loss,  $L(\hat{y}, y)$ . The model is typically composed of a set of computational layers parameterized in aggregate by weight parameters  $\theta$  giving us  $\hat{y} = f(x; \theta)$ . Assuming a purely feedforward model (a common form for image-based DNNs), we can decompose  $f$  as follows:

$$f(x; \theta) = f_L^{\theta_L} \circ f_{L-1}^{\theta_{L-1}} \circ \dots \circ f_2^{\theta_2} \circ f_1^{\theta_1}(x) = \hat{y} \quad (1)$$

where  $f_l^{\theta_l}(\cdot) = z_l$

Note that for machine vision problems,  $f(\cdot)$  is typically implemented as a convolutional neural network, whereby the intermediate layer activations,  $z_l$  may be 2D vectors or 3D tensors. Also, note that typically  $f(\cdot)$  produces an output that represents a distribution over the  $N$  classes where  $\hat{y} = \arg \max z_L$ . During a forward pass of our model, we record and aggregate all intermediate activations into  $\mathbf{z} = \{z_1, \dots, z_L\}$ .

### 5 THREAT MODEL

We define an adversarial example as a perturbation,  $\eta$ , such that for a correctly classified clean input (i.e.,  $f(x; \theta) = \hat{y} = y_{true}$ ), the added perturbation yields an incorrect classification (i.e.,  $f(x + \eta; \theta) = \hat{y} \neq y_{true}$ ). In a targeted case, the AE is constructed to cause  $\hat{y} = y_{target}$  whereas in an untargeted scenario, the AE is constructed to cause  $\hat{y} \neq y_{true}$ . In either case, the representation of the attacked image in feature space becomes shifted from its clean counterpart as illustrated in Figure 1.

In order to construct the most challenging detection task as possible from the perspective of the defender, we consider white-box scenarios whereby the attackers have full knowledge and access to the network weights and architecture to be attacked. In this setting, we assume that the attacker has access to the clean input and may modify it within specified constraints (e.g., a bound on the  $L_p$ -norm, i.e.,  $\|x - (x + \eta)\|_p \leq \epsilon$ ).

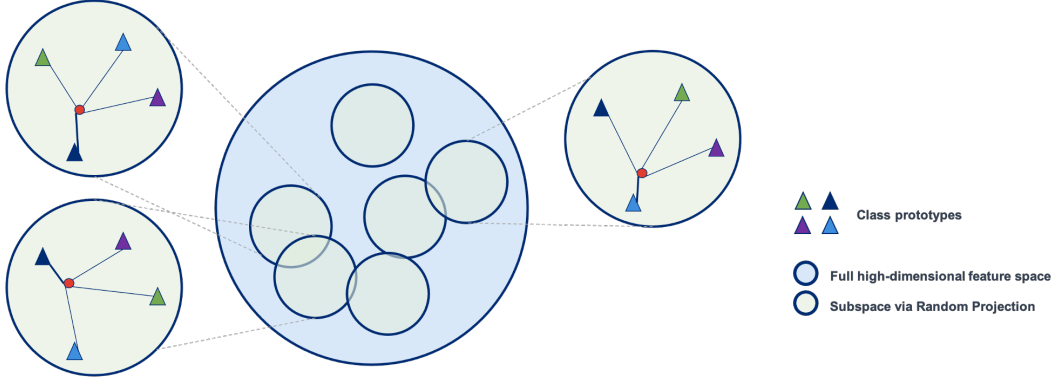


Figure 2: *Adversarial example detection via Random Subspace Analysis.* Random projections provide a mechanism for studying activation behavior with the aim to detect clean vs. adversarial examples. The likely existence of *non-robust but useful features* is exploited by measuring the consistency of the activation and latent space properties across multiple subspaces. Shown above, the two subspaces on the right are consistent with respect to which class prototype is closest to the test point. The rightmost subspace is inconsistent since a different colored class prototype is preferred.

## 6 ADVERSARIAL ATTACK DETECTION METHOD

### 6.1 DIMENSIONALITY REDUCTION VIA RANDOM PROJECTIONS

Recent work by Ilyas et al. (2019) provides compelling evidence for the existence of *robust* and *non-robust but useful features* which contribute to task performance but crucially, are informative regarding the susceptibility of the DNN to attacks. One possible mitigation strategy for adversarial manipulation of non-robust features is to perform dimensionality reduction of learned representations whereby the resulting features (most likely to be from the *robust* set) preserve classification-relevant information and reduce or remove the impact of manipulated features (most likely to be *non-robust*).

Conventional dimensionality reduction techniques (e.g., Principal Components Analysis, Singular Value Decomposition, Independent Component Analysis) offer principled approaches to achieving the reduction, but a primary disadvantage is that they are computationally expensive to compute in high-dimensions. Furthermore, while beneficial in many scenarios, these methods produce a single deterministic subspace which limits the scope for comparative analysis between properties of the reduced and full representations.

Instead, we turn to Random Projections (RP) which do not have the aforementioned drawbacks, provide many desirable properties (explained later), and allow for more flexible analysis. Our approach will be to project layer activations into a series of random subspaces and then compare the relation of these projections with respect to class prototypes (in each subspace). Differences between clean and adversarial behavior will be exploited to produce the final detection. Definitions of these terms and details will be discussed in the following sections.

We first define a random projection of activation  $z_i$  as:

$$z'_i = Rz_i \quad (2)$$

where  $R \in \mathbb{R}^{k \times d}$  ( $k \ll d$ ),  $z_i \in \mathbb{R}^d$ , and  $z'_i \in \mathbb{R}^k$ , elements of  $R$  are sampled independently from a normal distribution, and representations are extracted from layer  $i \in \{l \mid 1 \leq l \leq L\}$  of the DNN. Note that strictly speaking, the rows of  $R$  should be orthogonal. However, if  $R$ 's elements are sampled independently, it can be shown that the rows are approximately orthogonal and consequently the projections are reasonably approximate as well.

## 6.2 THEORETICAL CONSIDERATIONS

We draw particular motivation for using RP from the Johnson-Lindenstrauss Lemma which guarantees that with high probability, distances between pairs of points in the random subspace are preserved up to a scaling  $(1 \pm \epsilon)$ .

**Lemma 6.1 (Johnson-Lindenstrauss)** *Let  $X = \{x_1, \dots, x_k\}$  in  $\mathbb{R}^n$ . There exists a random function  $f : \mathbb{R}^n \rightarrow \mathbb{R}^m$  such that for any pair of points  $x_i, x_j$*

$$(1 - \epsilon)\|x_i - x_j\|_2^2 \leq \|f(x_i) - f(x_j)\|_2^2 \leq (1 + \epsilon)\|x_i - x_j\|_2^2 \quad (3)$$

with probability at least  $\frac{1}{k}$  so long as  $m \geq \frac{8 \log k}{\epsilon^2}$ .

The J-L Lemma is a statement about the existence of (random) embeddings in lower dimensions whereby the distortion of distances between a pair of points can be guaranteed to be limited. A proof of Lemma 6.1 can be found in Dasgupta & Gupta (1999). It is important to note that while the bound is tight, it represents a worst case scenario. In practice, distances are well-preserved below the theoretical value of  $m$  (see Bingham & Mannila (2001); Dasgupta (2013)). Prior work has also reported that RP can help preserve other aspects of geometry such as cluster separability (Dasgupta (2013)), volume, and distances to affine spaces (Magen (2002)), both theoretically and empirically. Connections between Restricted Isometry Property (RIP), a key ingredient for compressive sensing, and the J-L lemma were also made in Krahmer & Ward (2011).

## 6.3 RANDOM SUBSPACE ANALYSIS

Given the ability to reduce representation dimensionality while mostly preserving pairwise distances, our approach focuses on measuring the consistency of the local geometry between the ambient and subspace representations. In particular, we can leverage the ability to produce arbitrary random projections to analyze DNN activations in multiple subspaces derived from the original full-dimensional space (illustrated conceptually in Figure 2).

More formally, we can define  $M$  projections,  $\{R_m | 1 \leq m \leq M\}$  applied to activation  $z_l$  from layer  $l$ , and produce a set of subspace representations:

$$\mathbf{z}'_l = \{z'_{l,m}\} = \{R_m z_l | 1 \leq m \leq M\} \quad (4)$$

Because the RP preserves distances within some scaling, the loss of information can be advantageous. As evidenced by the nearest-neighbor type analyses (e.g., Papernot & McDaniel (2018)), adversarial features are likely to exhibit greater similarity to exemplars of the non-true class than the true class.

The potential distinction between robust and non-robust but useful features, suggests that some subset of features (namely the non-robust variety) may be more likely than others to be manipulated under attack. Under a set of random projections, the influence of the manipulated features on the final outcome becomes increased/decreased depending on the specific projection itself.

In the case that the manipulated features becomes less influential in the random subspace, then the projection should show greater similarity to examples of the true class than the incorrect classes. Conversely, if the manipulated features becomes more influential, then the projection should show greater dissimilarity with the true class representation. When examined over a set of random projections, inconsistent behavior is likely to be exposed and amplified. For clean examples, projections should exhibit strong overall self-consistency to the true class across a set of projections (as suggested by the J-L lemma).

To build our detection model, we first extract features  $z_l$  for each image  $x$  in a training dataset of clean images  $\mathcal{D}_T = \{(x, y) | x \in \mathcal{I}, y \in \{1, \dots, K\}\}$ . We compute class-conditional prototypes:

$$\hat{\mu}_{l,k} = \frac{1}{N_k} \sum_{i: y=k} f_l(x_i; \theta) \quad (5)$$

where  $N_k$  is the number of examples with label  $k$ . Then, as described in Algorithm 1, we project both the test point features and the prototypes into the same subspace, determine the nearest prototype in the subspace, and return the associated label for each layer of interest.

---

**Algorithm 1:** Random Subspace Analysis

---

**Result:** Random Subspace Analysis

**Input :**  $z_l$  : Activation for the test image at layer  $l$

$\hat{\mu}_l$  : Class prototypes (k-total) computed at layer  $l$

$R_l$  : Set of  $M$  random projection matrices for layer  $l$

$d(\cdot)$  : Distance function (i.e., euclidean, cosine)

**Output:**  $\hat{C}_l$  : Set of  $M$  predicted class labels (one for each RP)

1 Initialize the RP nearest-label array  $\hat{C}_l = []$ ;

2 **for**  $m \in \{1, \dots, M\}$  **do**

3     Initialize distances array  $D = []$ ;

4     Project activation:  $z'_l = R_m z_l$ ;

5     **for**  $k \in \{1, \dots, K\}$  **do**

6         Project prototype:  $\hat{\mu}'_{l,k} = R_m \hat{\mu}_{l,k}$ ;

7         Add  $d(z'_l, \hat{\mu}'_{l,k})$  to  $D$ ;

8     Add  $\hat{l}_m = \arg \min_k(D)$  to  $\hat{C}_l$ ;

9 **return**  $\hat{C}_l$ ;

---

#### 6.4 AE DETECTION

To piece everything together, we apply a simple decision rule on the nearest-prototype set (which captures the label of the nearest prototype to the test point in each subspace),  $\hat{C}_l$ , to predict whether the test point is adversarial (represented as  $\hat{a}$ ) and where  $\text{mode}(\hat{C}_l)$  represents the label occurring most frequently in  $\hat{C}_l$ .

$$\hat{a} = \begin{cases} 1 & \text{if } \frac{|\{c | c = \text{mode}(\hat{C}_l)\}|}{M} < \alpha \text{ for } \alpha \in [0, 1] \\ 0 & \text{otherwise} \end{cases} \quad (6)$$

Note that the set  $\hat{C}_l$  may be replaced by  $\hat{C}$  which is an aggregation of label preference across multiple layers of the network (i.e.,  $\hat{C} = \bigcup \hat{C}_l$  for  $l \in L' \subseteq L$ ). Essentially, 6 represents the fraction of label agreement across all random subspaces (as determined by the distance from the test point to its nearest prototype).

Of course, more powerful decision rules may be developed and employed, but the rule in (6) provides several notable advantages: (1) it is simple to compute, (2) it is tunable by a single hyperparameter  $\alpha$ , (3) it is agnostic to the ground-truth label, and (4) it is non-differentiable (increasing its robustness against many powerful attacks). Note that  $\alpha = 0$  corresponds to the degenerate case where  $x$  is labeled as clean in all cases whereas  $\alpha = 1$  is the most stringent case such that the label for the nearest-prototype must be the same for all random projections in order for  $x$  to be considered clean. To be truly attack agnostic, the selection of  $\alpha$  can be performed absent of any attack data (e.g., by requiring a certain degree of agreement across subspaces). However, if attack data is available,  $\alpha$  may be tuned in a more principled way.

Item (3) is of particular importance given that the true class is not known for new  $x$ , and thus we cannot condition the detection on the true label. While many methods condition the detection on the DNN's prediction  $\hat{y}$  (e.g., Papernot & McDaniel (2018); Ma et al. (2018c); Feinman et al. (2017)), our approach considers only whether the label of the nearest prototype stays consistent across random subspaces. Thus, we are able to use class-level representations while still separating AE detection from image classification. In essence, our method takes advantage of competing elements of adversarial attacks, namely changing the predicted label of the model without changing the true meaning of the input.

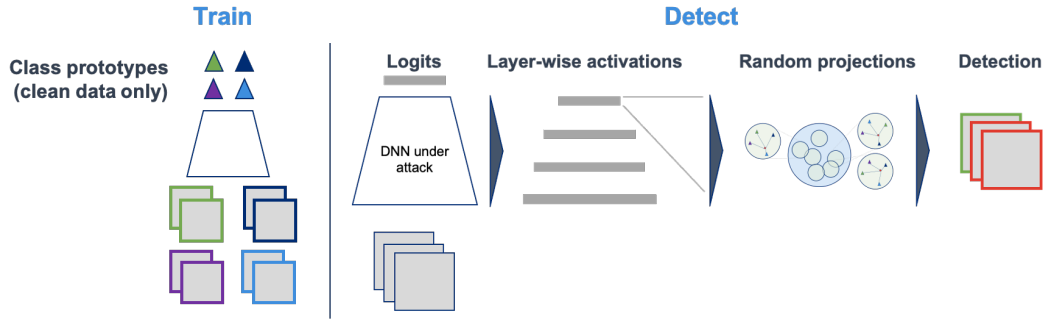


Figure 3: AE detection pipeline: During the training step, class prototypes are computed from clean data only (one prototype per class). At detection time, activations computed for the test images (gray squares) are projected to a set of random subspaces and consistency is measured in terms of label preference. The simplest detection rule applies a threshold to the label consistency measure.

## 7 DATA AND MODELS

### 7.1 ADVERSARIAL EXAMPLE GENERATION

To test our detection approach, we generated sets of (*clean*, *adversarial*) image pairs on which to evaluate. We make use of the Foolbox toolkit (Rauber et al. (2017)) to generate attacks with varying complexity and strategy, including FGSM (Goodfellow et al. (2014)), PGD (Madry et al. (2017)), CWL2 (Carlini & Wagner (2017)), JSMA (Papernot et al. (2016)), EAD (Chen et al. (2017)), and gradient-free noise).

We evaluate our detection approach (Figure 3) under a white-box threat model whereby the adversary has full knowledge of the network architecture and weights. Attack parameters are chosen to be consistent with those commonly found in the literature (which balance attack effectiveness and subtlety). This threat model provides an approximate lower-bound for detection given that the adversary should not be able to improve their attack under less-favorable conditions.

### 7.2 DATA

For each experiment, we generate a set of 4000 (*clean*, *adversarial*) image pairs for each attack under consideration. To fit our detection model, we reserve 10% of the clean examples for computing the class-specific prototypes and the remaining 90% of exemplars for evaluation.

For each attack, we follow standard practice for evaluating AE detection and evaluate only the (*clean*, *adversarial*) pairs where both elements achieve their objectives (i.e., correct classification, misclassification). For both cases, we aim to avoid confounding our detector’s performance with other data/model-related issues that would come from misclassification of clean examples or failed attempts to attack the model.

### 7.3 WHITE-BOX MODELS

We focus our efforts on attacking commonly used, high-performing architectures for image classification. We train Resnet[18,34] (He et al. (2016)) and DenseNet161 (Huang et al. (2017)) models from scratch on each dataset. We train for 200 epochs using SGD with a base learn rate of  $10^{-1}$  (decreasing by 0.1 every 50 epochs starting from epoch 100), momentum of 0.9, and weight decay constant of  $10^{-4}$ . These models are then used directly for the white-box attack generation to ensure the most challenging AE detection scenario.

### 7.4 BASELINES AND SOTA COMPARISONS

We compare our method against top performing baselines from Lee et al. (2018) and Ma et al. (2018c). We modify these approaches (referred to as DMD-OC and LID-OC respectively) to fit our

paradigm in two ways. First, we are primarily interested in attack-agnostic detection implying that we must have detection methods that do not require adversarial examples during the training step. As such, we replace the Logistic Regression classifiers in both methods with a One-Class Support Vector Machine (SVM) (Schölkopf et al. (2001)) trained only on clean activations. Second, we focus on a test paradigm where the training set is limited in size. While this restriction does not force us to alter the underlying methods themselves, we note that it will affect the overall quality of the detection results for these approaches given that they’re typically fit on much larger training sets.

## 8 EXPERIMENTS

In all of the following experiments, for simplicity, we run our detection method using the output from the last layer prior to the classification layer. However, future work could study in greater depth the impact of additional layers. Following standard practice, the primary performance metric is AUC score which allows us to sweep over decision thresholds (i.e.,  $\alpha$  for our method and similar for other baselines) rather than choose a potentially sub-optimal operating point.

### 8.1 WHITE-BOX ATTACKS

In this section we consider AE detection for untargeted white-box attacks. As our method is agnostic to the attack algorithm, we observe the detection performance across a range of attacks and consider the differences in performance between them. Table 1 illustrates the detection performance for untargeted attacks. In all cases,  $k = 16$  for the RP dimension,  $M = 8$  projections were used for the detector.

Dataset	Architecture	Detector	Attack					
			FGSM	PGD	JSMA	EAD	CWL2	Noise
CIFAR10	ResNet18	LID-OC	0.570	0.525	0.547	0.509	0.540	0.533
		DeepMD-OC	0.502	0.550	0.547	0.547	0.551	0.553
		DeepRP (ours)	<b>0.955</b>	<b>0.964</b>	<b>0.962</b>	<b>0.951</b>	<b>0.954</b>	<b>0.930</b>
	ResNet34	LID-OC	0.495	0.522	0.519	0.512	0.498	0.505
		DeepMD-OC	0.500	0.601	0.594	0.585	0.583	0.602
		DeepRP (ours)	<b>0.946</b>	<b>0.974</b>	<b>0.972</b>	<b>0.941</b>	<b>0.966</b>	<b>0.915</b>
	DenseNet161	LID-OC	0.491	0.496	0.533	0.493	0.486	0.553
		DeepMD-OC	0.500	0.500	0.500	0.500	0.500	0.500
		DeepRP (ours)	<b>0.928</b>	<b>0.926</b>	<b>0.931</b>	<b>0.920</b>	<b>0.926</b>	<b>0.952</b>
SVHN	ResNet18	LID-OC	0.601	0.482	0.480	0.487	0.468	0.299
		DeepMD-OC	0.501	0.603	0.569	0.603	0.584	0.571
		DeepRP (ours)	<b>0.954</b>	<b>0.957</b>	<b>0.965</b>	<b>0.951</b>	<b>0.952</b>	<b>0.950</b>
	ResNet34	LID-OC	0.543	0.509	0.514	0.494	0.475	0.384
		DeepMD-OC	0.507	0.591	0.580	0.595	0.592	0.577
		DeepRP (ours)	<b>0.953</b>	<b>0.937</b>	<b>0.956</b>	<b>0.944</b>	<b>0.944</b>	<b>0.923</b>
	DenseNet161	LID-OC	0.513	0.581	0.585	0.588	0.569	0.795
		DeepMD-OC	0.500	0.500	0.500	0.500	0.500	0.500
		DeepRP (ours)	<b>0.959</b>	<b>0.972</b>	<b>0.975</b>	<b>0.967</b>	<b>0.967</b>	<b>0.968</b>

Table 1: AUC score for detection of white-box untargeted perturbation attacks on CIFAR10 and SVHN. Best methods indicated in **bold**.

### 8.2 SENSITIVITY STUDIES

We run additional sensitivity studies to determine the impact of both the dimensionality of the random subspace as well as the number of subspaces considered during the detection process.

#### RP DIMENSION DEPENDENCY

Table 2 shows the impact of changing the dimension of the RP on the AE detection result. In all cases,  $M = 8$  projections were used for the layer prior to the final output layer. The full dimen-



sionality of the final layer is 512, so the subspace dimensions studied here represent a modest to aggressive reduction.

Dataset	Architecture	Detector	Attack					
			FGSM	PGD	JSMA	EAD	CWL2	Noise
CIFAR10	ResNet18	DeepRP-k8	0.935	0.948	0.947	0.940	0.928	<b>0.948</b>
		DeepRP-k16	0.955	<b>0.964</b>	<b>0.962</b>	<b>0.951</b>	<b>0.954</b>	0.930
		DeepRP-k32	<b>0.961</b>	0.959	0.961	0.943	0.945	0.901
		DeepRP-k64	0.952	0.958	0.945	0.926	0.931	0.843
		DeepRP-k128	0.910	0.918	0.904	0.855	0.873	0.752
SVHN	ResNet18	DeepRP-k8	0.953	<b>0.958</b>	<b>0.966</b>	<b>0.961</b>	<b>0.959</b>	<b>0.967</b>
		DeepRP-k16	<b>0.954</b>	0.957	0.965	0.951	0.952	0.950
		DeepRP-k32	0.934	0.916	0.943	0.909	0.922	0.904
		DeepRP-k64	0.877	0.845	0.879	0.838	0.848	0.834
		DeepRP-k128	0.824	0.779	0.811	0.775	0.783	0.768

Table 2: AUC score for detection of white-box untargeted perturbation attacks on CIFAR10, SVHN as the dimension of the RP changes. Best results indicated in **bold face**.

#### DEPENDENCE ON NUMBER OF PROJECTIONS

Table 3 captures the impact of the number of projections,  $M$ , considered at detection time. We fix the dimensionality to  $k = 16$ . We focus here on a range of projections to capture the tradeoff between having sufficient data for measuring label consistency and over-inflating the computational requirements for performing detection.

Dataset	Architecture	Detector	Attack					
			FGSM	PGD	JSMA	EAD	CWL2	Noise
CIFAR10	ResNet18	DeepRP-M2	0.768	0.770	0.771	0.750	0.764	0.786
		DeepRP-M4	0.895	0.911	0.910	0.889	0.904	0.891
		DeepRP-M8	0.955	0.964	0.962	0.951	0.954	0.930
		DeepRP-M16	0.968	0.976	0.974	0.966	0.965	0.953
		DeepRP-M32	<b>0.974</b>	<b>0.980</b>	<b>0.980</b>	<b>0.971</b>	<b>0.970</b>	<b>0.966</b>
SVHN	ResNet18	DeepRP-M2	0.767	0.753	0.770	0.761	0.767	0.823
		DeepRP-M4	0.904	0.901	0.920	0.894	0.895	0.910
		DeepRP-M8	0.954	0.957	0.965	0.951	0.952	0.950
		DeepRP-M16	0.966	0.972	0.974	0.964	0.967	0.960
		DeepRP-M32	<b>0.970</b>	<b>0.977</b>	<b>0.979</b>	<b>0.972</b>	<b>0.976</b>	<b>0.971</b>

Table 3: AUC score for detection of white-box untargeted perturbation attacks on CIFAR10, SVHN as the dimension of the RP changes. Best results indicated in **bold face**.

#### EXPANDED TRAINING DATA

We perform additional experiments which increase the amount of clean-only training data available to the detectors and present them in Table 4. Since the detectors are only fit to clean data and due to the limited size of the train/test splits for detection, we expand the available data by drawing from the original training set (which was used only for training the core model). While this is not common practice, this approach still has practical value since it allows the detectors to use the embeddings the network was directly trained to produce. Data used for detection is held out as normal.

These results suggest that the strength of other detection methods scales in proportion to the available training data whereas our method provides consistent performance for small and larger training set sizes.

#### 8.3 EXPERIMENTS ON MINI-IMAGENET

We run additional experiments on mini-ImageNet to test the effectiveness of our method on more challenging data (Table 5). We focus on scaling the complexity of the detection task to the image data itself (higher resolution, greater diversity) rather than the classification task itself (e.g., more

Dataset	Architecture	Detector	Attack				
			FGSM	PGD	JSMA	CWL2	Noise
CIFAR10	ResNet18	LID-OC	0.495	0.525	0.525	0.535	0.763
		DeepMD-OC	0.833	0.864	0.885	0.860	0.849
		DeepRP (ours)	<b>0.961</b>	<b>0.966</b>	<b>0.963</b>	<b>0.957</b>	<b>0.948</b>
	ResNet34	LID-OC	0.486	0.493	0.584	0.556	0.739
		DeepMD-OC	0.837	0.899	0.904	0.902	0.861
		DeepRP (ours)	<b>0.965</b>	<b>0.973</b>	<b>0.971</b>	<b>0.967</b>	<b>0.928</b>

Table 4: AUC score for detection of white-box untargeted perturbation attacks on CIFAR10 for 10x more training data. Best methods indicated in **bold face**.

classes). For these experiments, we choose the DeepRP hyperparameters to be  $M = 32$  and  $k = 16$ . We also expand the training dataset to be 2000 clean examples.

Results show that our method far outperforms all competing methods even as the images become more complex in terms of resolution and statistics. That said, we believe that the difficulty of the ImageNet data relative to CIFAR or SVHN motivates a greater expansion of the training dataset to get more stable estimates of the class prototypes which will ultimately affect the detection performance.

Dataset	Architecture	Detector	Attack					
			FGSM	PGD	JSMA	EAD	CWL2	Noise
mini-ImageNet	ResNet18	LID-OC	0.533	0.537	0.502	0.524	0.528	0.498
		DeepMD-OC	0.449	0.472	0.476	0.470	0.464	0.558
		DeepRP (ours)	<b>0.790</b>	<b>0.760</b>	<b>0.749</b>	<b>0.744</b>	<b>0.760</b>	<b>0.871</b>

Table 5: AUC score for detection of white-box untargeted perturbation attacks on mini-Imagenet for 2k clean examples for training. Best methods indicated in **bold face**.

## 9 DISCUSSION

The results of our experiments demonstrate the efficacy of our approach and leads to several key observations. First, we note that the overall detection performance of our method is consistently high across attack algorithms, demonstrating a relative independence between our detection method and the details of attack (under the same threat model). We observe slight differences between the detection performance given the model type under attack, but note that even then, the detection performance is consistent.

We also highlight that our method outperforms the other baselines under this more rigorous paradigm. The main performance difference can be mostly attributed to the significant reduction in the training set size. While our method as well as these baselines would benefit greatly from having more training data (i.e., to produce more stable prototypes (ours), reduce the sparsity of the latent space (LID), improve the mean/covariance estimates (DMD)), results indicate that our approach is considerably more robust under this constraint. This lends credence to the use of our approach under a greater range of conditions where the attack is unknown and available training data may be limited.

Tables 2 and 3 indicate some dependence both on the dimension of the random project ( $k$ ) and the number of projections considered during the detection process ( $M$ ). In both cases, there is a clear tradespace whereby an appropriate balance must be struck for  $k$  and  $M$ . For  $k$ , results suggest that the RP must perform a certain degree of compression, but too little results in a representation that is too similar to the original (i.e., inclusion of too many non-robust features) and too much results in a significant loss of information (i.e., loss of robust and non-robust features). For  $M$ , the balance must be between too few subspaces under consideration (resulting in insufficient observations of activation behavior) and too many (where subspace diversity becomes less prominent).

We also note that the additive noise attack produces, in general, the lowest detection performance. Since this attack requires no knowledge of the underlying model architecture or weights, it is unable to preferentially target (implicitly or explicitly) the non-robust features over the robust ones. As such, the random subspaces are more likely to produce consistent behavior and thereby miss

---

possible detections. While this attack is notably weak compared to more sophisticated approaches (e.g., Carlini & Wagner (2017)), it highlights how an adaptive adversary might attempt to circumvent our detection scheme. However, while modifying an attack to more evenly manipulate features may evade detection, it may have unintended and detrimental consequences on the overall viability of the attack itself. We leave it to future work to investigate this tradespace of competing objectives in more depth.

## 10 CONCLUSIONS

We present a novel approach to adversarial example detection via random subspace analysis. We use random projections to reduce dimensionality of deep features and then examine the consistency of features across a set of subspaces to detect attacks. We evaluate our method under much more rigorous constraints than prior approaches by constraining the training set to clean examples only and further restricting the amount of training data available.

Our results demonstrate that our approach, while being attack agnostic, consistently outperforms against a range of SOTA attack strategies with various degrees of sophistication. We believe that this work opens up new approaches for analyzing deep features in the context of adversarial example detection via random subspace analysis.

## REFERENCES

- Tarek Abdelzaher, Nora Ayanian, Tamer Basar, Suhas Diggavi, Jana Diesner, Deepak Ganesan, Ramesh Govindan, Susmit Jha, Tancrede Lepoint, Benjamin Marlin, et al. Toward an internet of battlefield things: A resilience perspective. *Computer*, 51(11):24–36, 2018.
- Alexander Bagnall, Razvan Bunescu, and Gordon Stewart. Training ensembles to detect adversarial examples. *arXiv preprint arXiv:1712.04006*, 2017.
- Ella Bingham and Heikki Mannila. Random projection in dimensionality reduction: applications to image and text data. In *Proceedings of the seventh ACM SIGKDD international conference on Knowledge discovery and data mining*, pp. 245–250, 2001.
- Akhilan Boopathy, Tsui-Wei Weng, Pin-Yu Chen, Sijia Liu, and Luca Daniel. Cnn-cert: An efficient framework for certifying robustness of convolutional neural networks. In *Proceedings of the AAAI Conference on Artificial Intelligence*, volume 33, pp. 3240–3247, 2019.
- Nicholas Carlini and David Wagner. Towards evaluating the robustness of neural networks. In *2017 IEEE Symposium on Security and Privacy (SP)*, pp. 39–57. IEEE, 2017.
- Pin-Yu Chen, Yash Sharma, Huan Zhang, Jinfeng Yi, and Cho-Jui Hsieh. Ead: elastic-net attacks to deep neural networks via adversarial examples. *arXiv preprint arXiv:1709.04114*, 2017.
- F Crecchi, D Bacciu, and B Biggio. Detecting adversarial examples through nonlinear dimensionality reduction. In *27th European Symposium on Artificial Neural Networks, Computational Intelligence and Machine Learning, ESANN 2019*, pp. 483–488. ESANN (i6doc. com), 2019.
- Sanjoy Dasgupta. Experiments with random projection. *arXiv preprint arXiv:1301.3849*, 2013.
- Sanjoy Dasgupta and Anupam Gupta. An elementary proof of the johnson-lindenstrauss lemma. *International Computer Science Institute, Technical Report*, 22(1):1–5, 1999.
- Reuben Feinman, Ryan R Curtin, Saurabh Shintre, and Andrew B Gardner. Detecting adversarial samples from artifacts. *arXiv preprint arXiv:1703.00410*, 2017.
- Gil Fidel, Ron Bitton, and Asaf Shabtai. When explainability meets adversarial learning: Detecting adversarial examples using shap signatures. *arXiv preprint arXiv:1909.03418*, 2019.
- Timon Gehr, Matthew Mirman, Dana Drachler-Cohen, Petar Tsankov, Swarat Chaudhuri, and Martin Vechev. Ai2: Safety and robustness certification of neural networks with abstract interpretation. In *2018 IEEE Symposium on Security and Privacy (SP)*, pp. 3–18. IEEE, 2018.

- 
- Ian J Goodfellow, Jonathon Shlens, and Christian Szegedy. Explaining and harnessing adversarial examples. *arXiv preprint arXiv:1412.6572*, 2014.
- Kathrin Grosse, Praveen Manoharan, Nicolas Papernot, Michael Backes, and Patrick McDaniel. On the (statistical) detection of adversarial examples. *arXiv preprint arXiv:1702.06280*, 2017.
- Kaiming He, Xiangyu Zhang, Shaoqing Ren, and Jian Sun. Deep residual learning for image recognition. In *Proceedings of the IEEE conference on computer vision and pattern recognition*, pp. 770–778, 2016.
- Gao Huang, Zhuang Liu, Laurens Van Der Maaten, and Kilian Q Weinberger. Densely connected convolutional networks. In *Proceedings of the IEEE conference on computer vision and pattern recognition*, pp. 4700–4708, 2017.
- Andrew Ilyas, Shibani Santurkar, Dimitris Tsipras, Logan Engstrom, Brandon Tran, and Aleksander Madry. Adversarial examples are not bugs, they are features. In *Advances in Neural Information Processing Systems*, pp. 125–136, 2019.
- Felix Krahmer and Rachel Ward. New and improved johnson–lindenstrauss embeddings via the restricted isometry property. *SIAM Journal on Mathematical Analysis*, 43(3):1269–1281, 2011.
- Aounon Kumar, Alexander Levine, Tom Goldstein, and Soheil Feizi. Curse of dimensionality on randomized smoothing for certifiable robustness. *arXiv preprint arXiv:2002.03239*, 2020.
- Mathias Lecuyer, Vaggelis Atlidakis, Roxana Geambasu, Daniel Hsu, and Suman Jana. Certified robustness to adversarial examples with differential privacy. In *2019 IEEE Symposium on Security and Privacy (SP)*, pp. 656–672. IEEE, 2019.
- Kimin Lee, Kibok Lee, Honglak Lee, and Jinwoo Shin. A simple unified framework for detecting out-of-distribution samples and adversarial attacks. In *Advances in Neural Information Processing Systems*, pp. 7167–7177, 2018.
- Alexander Levine and Soheil Feizi. Wasserstein smoothing: Certified robustness against wasserstein adversarial attacks. *arXiv preprint arXiv:1910.10783*, 2019.
- Xin Li and Fuxin Li. Adversarial examples detection in deep networks with convolutional filter statistics. In *Proceedings of the IEEE International Conference on Computer Vision*, pp. 5764–5772, 2017.
- Bin Liang, Hongcheng Li, Miaoqiang Su, Xirong Li, Wenchang Shi, and Xiaofeng Wang. Detecting adversarial image examples in deep neural networks with adaptive noise reduction. *IEEE Transactions on Dependable and Secure Computing*, 2018.
- Zhaoyang Lyu, Ching-Yun Ko, Zhifeng Kong, Ngai Wong, Dahua Lin, and Luca Daniel. Fastened crown: Tightened neural network robustness certificates. *arXiv preprint arXiv:1912.00574*, 2019.
- Lei Ma, Felix Juefei-Xu, Fuyuan Zhang, Jiyuan Sun, Minhui Xue, Bo Li, Chunyang Chen, Ting Su, Li Li, Yang Liu, et al. Deepgauge: Multi-granularity testing criteria for deep learning systems. In *Proceedings of the 33rd ACM/IEEE International Conference on Automated Software Engineering*, pp. 120–131, 2018a.
- Lei Ma, Fuyuan Zhang, Minhui Xue, Bo Li, Yang Liu, Jianjun Zhao, and Yadong Wang. Combinatorial testing for deep learning systems. *arXiv preprint arXiv:1806.07723*, 2018b.
- Xingjun Ma, Bo Li, Yisen Wang, Sarah M Erfani, Sudanthi Wijewickrema, Grant Schoenebeck, Dawn Song, Michael E Houle, and James Bailey. Characterizing adversarial subspaces using local intrinsic dimensionality. *arXiv preprint arXiv:1801.02613*, 2018c.
- Aleksander Madry, Aleksandar Makelov, Ludwig Schmidt, Dimitris Tsipras, and Adrian Vladu. Towards deep learning models resistant to adversarial attacks. *arXiv preprint arXiv:1706.06083*, 2017.
- Avner Magen. Dimensionality reductions that preserve volumes and distance to affine spaces, and their algorithmic applications. In *International Workshop on Randomization and Approximation Techniques in Computer Science*, pp. 239–253. Springer, 2002.

- 
- Jan Hendrik Metzen, Tim Genewein, Volker Fischer, and Bastian Bischoff. On detecting adversarial perturbations. *arXiv preprint arXiv:1702.04267*, 2017.
- David J Miller, Yulia Wang, and George Kesidis. When not to classify: Anomaly detection of attacks (ada) on dnn classifiers at test time. *arXiv preprint arXiv:1712.06646*, 2017.
- Nicolas Papernot and Patrick McDaniel. Deep k-nearest neighbors: Towards confident, interpretable and robust deep learning. *arXiv preprint arXiv:1803.04765*, 2018.
- Nicolas Papernot, Patrick McDaniel, Somesh Jha, Matt Fredrikson, Z Berkay Celik, and Ananthram Swami. The limitations of deep learning in adversarial settings. In *2016 IEEE European symposium on security and privacy (EuroS&P)*, pp. 372–387. IEEE, 2016.
- Kexin Pei, Yinzhao Cao, Junfeng Yang, and Suman Jana. Deepxplore: Automated whitebox testing of deep learning systems. In *proceedings of the 26th Symposium on Operating Systems Principles*, pp. 1–18, 2017.
- Igor M Quintanilha, Roberto de ME Filho, José Lezama, Mauricio Delbracio, and Leonardo O Nunes. Detecting out-of-distribution samples using low-order deep features statistics. 2018.
- Aditi Raghunathan, Jacob Steinhardt, and Percy Liang. Certified defenses against adversarial examples. *arXiv preprint arXiv:1801.09344*, 2018.
- Jonas Rauber, Wieland Brendel, and Matthias Bethge. Foolbox: A python toolbox to benchmark the robustness of machine learning models. *arXiv preprint arXiv:1707.04131*, 2017.
- Kevin Roth, Yannic Kilcher, and Thomas Hofmann. The odds are odd: A statistical test for detecting adversarial examples. In *International Conference on Machine Learning*, pp. 5498–5507, 2019.
- Bernhard Schölkopf, John C Platt, John Shawe-Taylor, Alex J Smola, and Robert C Williamson. Estimating the support of a high-dimensional distribution. *Neural computation*, 13(7):1443–1471, 2001.
- Sahil Singla and Soheil Feizi. Robustness certificates against adversarial examples for relu networks. *arXiv preprint arXiv:1902.01235*, 2019.
- Youcheng Sun, Xiaowei Huang, Daniel Kroening, James Sharp, Matthew Hill, and Rob Ashmore. Testing deep neural networks. *arXiv preprint arXiv:1803.04792*, 2018a.
- Youcheng Sun, Min Wu, Wenjie Ruan, Xiaowei Huang, Marta Kwiatkowska, and Daniel Kroening. Concolic testing for deep neural networks. In *Proceedings of the 33rd ACM/IEEE International Conference on Automated Software Engineering*, pp. 109–119, 2018b.
- Shixin Tian, Guolei Yang, and Ying Cai. Detecting adversarial examples through image transformation. In *Thirty-Second AAAI Conference on Artificial Intelligence*, 2018.
- Lu Wang, Xuanqing Liu, Jinfeng Yi, Zhi-Hua Zhou, and Cho-Jui Hsieh. Evaluating the robustness of nearest neighbor classifiers: A primal-dual perspective. *arXiv preprint arXiv:1906.03972*, 2019.
- Lily Weng, Huan Zhang, Hongge Chen, Zhao Song, Cho-Jui Hsieh, Luca Daniel, Duane Boning, and Inderjit Dhillon. Towards fast computation of certified robustness for relu networks. In *International Conference on Machine Learning*, pp. 5276–5285, 2018.
- Lily Weng, Pin-Yu Chen, Lam Nguyen, Mark Squillante, Akhilan Boopathy, Ivan Oseledets, and Luca Daniel. Proven: Verifying robustness of neural networks with a probabilistic approach. In *International Conference on Machine Learning*, pp. 6727–6736, 2019.
- Eric Wong and Zico Kolter. Provable defenses against adversarial examples via the convex outer adversarial polytope. In *International Conference on Machine Learning*, pp. 5286–5295, 2018.
- Weilin Xu, David Evans, and Yanjun Qi. Feature squeezing: Detecting adversarial examples in deep neural networks. *arXiv preprint arXiv:1704.01155*, 2017.